ILASS-Americas 31st Annual Conference on Liquid Atomization and Spray Systems, Madison, WI, May 2020

A Maximum-Entropy-Formalism for Secondary Droplet Breakup

C.W. Kuo and M.F. Trujillo*
Department of Mechanical Engineering
University of Wisconsin - Madison
Madison, WI 53706 USA

Abstract

In Lagrangian-Eulerian spray simulations, the secondary breakup of the atomized droplets is typically handled by an atomization model, such as the Kelvin-Helmholtz Rayleigh-Taylor model (1999 *Atomization and Sprays* **9**(6)) or the Taylor Analogy Breakup model (1987 *SAE Technical Paper*). This problem is revisited in this paper by imposing a joint probability density function (JPDF) over the size and velocity spaces of the droplets and enforcing the conservation constraints of mass, momentum, and energy. Five different models are proposed and tested. In the first three models, the size distribution is given in the form of the Nukiyama-Tanasawa, diameter-dependent Rosin-Rammler, and mass-dependent Rosin-Rammler distributions. For droplet velocity, a Dirac delta function centered on the parent droplet is assumed. The results show poor agreement with the experimental measurements. The next two models are based on the Maximum Entropy Methodology (MEM), which is contingent upon maximizing the Shannon entropy of the JPDF. In the first MEM model, the MEM is only applied to the size distribution while the velocity distribution is assumed to be a Dirac delta function. In the second MEM model, the size and velocity distributions are assumed to be fully coupled. Only the second MEM model agrees with the experimental measurements over a wide range of Weber numbers. Also, the second MEM model confirms the expected trend of a reduction of droplet size as the degree of droplet breakup intensity increases.

*Corresponding Author: mtrujillo@wisc.edu

1 Introduction

Due to its wide-ranging industrial applications, such as spray combustion [1, 2], fire suppression [3, 4], and agrochemicals [5, 6], predicting the droplet size statistics from the secondary breakup of the unstable liquid elements in the spray, known as secondary droplet atomization, is a long-standing subject of research. The Lagrangian-Eulerian (LE) models (e.g. [7], [8], [9]) is a particular means of exploring such problems, due in part to its straightforward application to constituting a realistic spray configuration.

In the LE framework, the gas phase is treated as a continuous phase and resolved in the Eulerian framework. The liquid phase is treated as a group of discrete liquid blobs. The breakup of a blob into droplets is then modeled through Lagrangian droplets. Attempts to successfully estimate droplet size within this context have resulted in various methods. Among these, the Kelvin-Helmholtz Rayleigh-Taylor model (the KH-RT model) [7] has received considerable attention as a viable option for simulating flows involving an intensive level of atomization severity. The KH-RT model employs the Kelvin-Helmholtz instability to describe the instability of the surface of the intact liquid core, and Rayleigh-Taylor instability to the surfaces of the atomized droplets, which, together with empirical coefficients, yields the average droplet size. Employing the Rosin-Rammler empirical function [10] then produces the droplet size distribution. The other route in estimating the droplet size is the Taylor Analogy Breakup model [8] (the TAB model), whose principal interest lies in the Taylor analogy between a damped/forced harmonic oscillator and an oscillating/distorting droplet. In line with this mean value, the droplet size is then randomly chosen from a Chi-square distribution [11].

Another attractive means of predicting droplet size statistics is to use a theoretically based approach of the maximum entropy method (MEM) advanced by Sellens and Brzustowski [12] as well as Li and Tankin [13]. In their works, they employ the Shannon entropy (S), which serves as a measure of the information produced when one message is selected from possible messages [14], and which is analogous to the Gibbs entropy in the statistical thermodynamics, for predicting the droplet size and/or velocity distributions in the spray. In accordance with such a relationship, and with appropriate conservation constraints of droplet properties, they found that the most probable droplet state after the breakup is the one in which the measure of the Shannon entropy reaches the maximum value.

The early work of the MEM method is targeted for sprays, in which the time required to complete a breakup event is relatively long. Accordingly, a source term is typically included in the conservation equations of droplet momentum and energy, accounting for the momentum loss and energy dissipation during atomization. Attempts at employing the MEM formalism to the spectrum of atomization problems, with attention being paid to the modeling of the source terms, have led to disparate MEM models (e.g. [15, 16, 17]).

For the secondary atomization of droplets, the breakup time is relatively short. This raises the question as to whether the inclusion of the source term to the MEM model is appropriate, among other things. Surveying the literature suggests that this topic has largely been neglected in previous studies on the MEM. To the best knowledge of the authors, only the paper by Bodaghkhani et al. [18] employs the MEM method for secondary droplet atomization. However, they still include the source terms in their analysis, although the source terms are modified in line with the specifications of the droplet breakup.

In response to the limited studies on MEM secondary-breakup models, this paper sets out to fashion a MEM-based model for calculating the distribution of the secondary droplets The model will be compared and contrasted with another MEM model which is derived under certain simplified conditions and other analytical models which inherit the formulations of the empirical distributions.

2 Derivation of droplet breakup models

We assume that the moving direction of the droplets after the breakup remains unchanged. The conservations of mass, momentum, and total energy for a breakup event q of a droplet, which at the precise moment of breakup has the following relationship

$$(1/6)\pi\rho_L \sum_{i=1}^{N_q} D_i^3 = (1/6)\pi\rho_L D_o^3 \tag{1}$$

$$(1/6)\pi\rho_L \sum_{i=1}^{N_q} D_i^3 u_i = (1/6)\pi\rho_L D_o^3 u_o \tag{2}$$

$$\begin{aligned}(1/12)\pi\rho_L \sum_{i=1}^{N_q} D_i^3 u_i^2 + \sigma\pi \sum_{i=1}^{N_q} D_i^2 \\ = (1/12)\pi\rho_L D_o^3 u_o^2 + \sigma\pi D_o^2\end{aligned} \tag{3}$$

where ρ_L is the droplet density, D_o is the diameter of the parent droplet, u_o is the velocity magnitude

of the parent droplet in a direction of travel relative to the gas, and σ is the surface tension coefficient. Furthermore, N_q is the number of secondary droplets generated per breakup event of realization q.

Taking an ensemble average for Eqs. 1 - 3 yields

$$\frac{1}{6}\pi\rho_L\left\langle \sum_{i=1}^{N_q} D_i^3 \right\rangle = \frac{1}{6}\pi\rho_L D_o^3 \tag{4}$$

$$\frac{1}{6}\pi\rho_L\left\langle \sum_{i=1}^{N_q} D_i^3 u_i \right\rangle = \frac{1}{6}\pi\rho_L D_o^3 u_o \tag{5}$$

$$\frac{1}{12}\pi\rho_L\left\langle \sum_{i=1}^{N_q} D_i^3 u_i^2 \right\rangle + \sigma\pi\left\langle \sum_{i=1}^{N_q} D_i^2 \right\rangle = \frac{1}{12}\pi\rho_L D_o^3 u_o^2 + \sigma\pi D_o^2 \tag{6}$$

The characteristics of the parent droplet do not change from one realization to another; hence, only the quantities on the LHS of Eqs. 4 - 6 change. To facilitate their description, we define a joint probability density function (JPDF). The JPDF is denoted by $f_{Du}(D,u)$, which is a continuous function whose value at the point (D, u) is the relative likelihood of finding the droplet of diameter D and velocity u.

We can define a general moment by f_{Du}

$$\langle D^r u^s \rangle = \int\limits_{\Omega_D\cup\Omega_u} (D^r u^s) f_{Du} dDdu \tag{7}$$

with r and s being integers, which, together with the following equivalency between the expected values

$$\langle D^r u^s \rangle = \frac{1}{\langle N_q \rangle}\left\langle \sum_{i=1}^{N_q} D_i^r u_i^s \right\rangle \tag{8}$$

allows us to write

$$\left\langle \sum_{i=1}^{N_q} D_i^r u_i^s \right\rangle = \langle N_q \rangle \int\limits_{\Omega_D\cup\Omega_u} (D^r u^s) f_{Du} dDdu \tag{9}$$

Substituting Eq. 9 into Eqs. 4 - 6, and after some manipulations, we have

$$\int\limits_{\Omega_D\cup\Omega_u} f_{Du}\frac{D^3}{D_{30}^3} dDdu = 1 \tag{10}$$

$$\int\limits_{\Omega_D\cup\Omega_u} f_{Du}\frac{D^3 u}{D_{30}^3 u_o} dDdu = 1 \tag{11}$$

$$\int\limits_{\Omega_D\cup\Omega_u} f_{Du}\left(\frac{D^3u^2}{D_{30}^3u_0^2} + \frac{12}{We_{Lo}}\frac{D_o}{D_{30}}\frac{D^2}{D_{30}^2}\right) dDdu = 1 + \frac{12}{We_{L,30}} \tag{12}$$

where $We_{L,30} = (\rho_L u_o^2 D_{30})/\sigma$ is the liquid-density-based Weber number relating to the mass mean diameter, D_{30}. The definition of D_{30} is

$$D_{30} = \left[\frac{\int_{\Omega_D} D^3 f_D dD}{\int_{\Omega_D} D^0 f_D dD}\right]^{1/3} \cong \left[\frac{D_o^3}{\langle N_q \rangle}\right]^{1/3} \tag{13}$$

where $\langle N_q \rangle$ is the expected value of N_q.

Eqs. 10 - 12 along with the normalization requirement of f_{Du}

$$\int\limits_{\Omega_D\cup\Omega_u} f_{Du} dDdu = 1 \tag{14}$$

constitute a set of constrains according to which the JPDF has to satisfy. In line with such constraints, five different models pertaining to the formulation of the JPDF will be derived and tested.

2.1 The Nukiyama-Tanasawa-based model (referred to as NT)

We assume that f_{Du} is related to the droplet size distribution $f_D(D)$ by the following relationship

$$f_{Du} = f_D(D)\delta(u) \tag{15}$$

where $f_D(D)$ is given in the form of the Nukiyama-Tanasawa empirical distribution [19]

$$f(D) = C_1 D^2 \exp\left(-C_2 - C_3 D^3\right) \tag{16}$$

and where C_1, C_2, and C_3 are the unknown constants which need to be solved. In addition, $\delta(u)$ is the Dirac delta function centered at the parent droplet (i.e. there is no change in the droplet velocity after breakup):

$$\delta(u) = \frac{1}{2\pi}\int\limits_{-\infty}^{\infty} e^{iku} dk \tag{17}$$

In this manner, Eq. 11 is reduced to Eq. 10. Meanwhile, Eq. 12 is simplified as:

$$\int\limits_{\Omega_D\cup\Omega_u} f_{Du}\frac{D_o}{D_{30}}\frac{D^2}{D_{30}^2} dDdu = 1 \tag{18}$$

We first solve C_1 and C_2. This is done by putting Eq. 15 - 17 into Eqs. 14 and 10, yielding $C_1 = 3C_3$ and $C_2 = -\ln\left(D_{30}^3 C_3\right)$. The estimation of

D_{30} follows Eq. 13, together with an empirical correlation of $\langle N_q \rangle$ (which is obtained by curve-fitting to Jain and colleagues' simulation data [20], and is calibrated with Kim et al.'s experimental measurements [15]). This is given as

$$D_{30} = \frac{D_o}{(5.5392 We_G^{2.2207})^{1/3}} \tag{19}$$

where $We_G = (\rho_G u_o^2 D_o)/\sigma$ is the gas-density-based Weber number.

With regards to C_3, it is obtained by putting Eq. 15 - 17 into Eq. 18, which, along with the known expressions of C_1 and C_2 as functions of C_3, yields $C_3 = 1/\{D_{32}^3[\Gamma_m(5/3)]^3\}$. Here, $\Gamma_m(n)$ is the gamma function, $\Gamma_m(n) = \int_0^\infty \exp(-x)x^{(n-1)}dx$, and D_{32} is the Sauter mean diameter.

The estimation of D_{32} is given by decomposing D_{32} into

$$D_{32} = \frac{D_{32}}{MMD}\frac{MMD}{D_{30}} \tag{20}$$

where the value of (MMD/D_{32}) is given as 1.2 [21]. The fraction MMD/D_{30} is obtained by combining the two empirical correlations provided by Monaghan et al. [22], yielding $MMD/D_{30} = 1.61$.

The model is given as:

$$f_D = \frac{3D^2}{[\Gamma_m(\frac{5}{3})]^3 D_{32}^3} \exp\left[\ln\left\{\frac{D_{30}^3/D_{32}^3}{[\Gamma_m(\frac{5}{3})]^3}\right\} - \frac{D^3/D_{32}^3}{[\Gamma_m(\frac{5}{3})]^3}\right] \tag{21}$$

2.2 The diameter-dependent Rosin-Rammler-based model (referred to as RR (dia))

Like the case of the first model, we begin by employing Eq. 15, yet with F_D being given in the form of the diameter-dependent Rosin-Rammler function [23]

$$f_D = \frac{n}{m\Gamma_m(\frac{n-3}{n})}\Big(\frac{D}{m}\Big)^{n-4} \exp\Big[-\Big(\frac{D}{m}\Big)^n\Big] \tag{22}$$

where m and n are the unknown parameters.

Once more, we assume that the droplet velocity distribution follows the Delta function. In line with this assumption, and due to the fact that Eq. 22 inherently satisfies the normalization constraint [23], the solutions of m and n are obtained by satisfying Eq. 10 and Eq. 18. This leads to two nonlinear equations. Solving both equations numerically then yields the solutions of m and n.

2.3 The mass-dependent Rosin-Rammler-based model (referred to as RR (mass))

The third model is similar to the second model, yet with f_D being given in the form the mass-dependent Rosin-Rammler function [23]

$$f_D(D) = \frac{n}{m}\Big(\frac{D}{m}\Big)^{n-1} \exp\Big[-\Big(\frac{D}{m}\Big)^n\Big] \tag{23}$$

where m and n are the unknown parameters. Like Eq. 22, Eq. 23 has shown to be matched with the normalization constraint [23], so m and n are again determined by satisfying Eq. 10 and Eq. 18. This is given as:

$$f_D(D) = \frac{3}{\Gamma_m(\frac{5}{3})D_{32}}\left[\frac{D/D_{32}}{\Gamma_m(\frac{5}{3})}\right]^2 \exp\Big[-\Big(\frac{D/D_{32}}{\Gamma_m(\frac{5}{3})}\Big)^3\Big] \tag{24}$$

2.4 The three-Lagrange-multiplier MEM model (referred to as MEM (3-Lag))

According to the MEM, and along with the Boltzmann's constant (k_B), the most probable droplet state after breakup, P_j, is the one in which the measure of the Shannon entropy (S) [14]

$$S = -k_B \sum_{j=0}^{n} P_j \ln P_j \tag{25}$$

reaches the maximum value in line with m conservation constraints and the normalization constraint of P_j:

$$\sum_{j=0}^{n} P_j = 1 \tag{26}$$

Here, k_B is the Boltzmann constant.

We assume that f_{Du} is the continuous counterpart of P_j. Accordingly, we put the Shannon entropy in continuous form, and so P_j can be approximated as f_{Du}:

$$S = -k_B \int\limits_{\Omega_D \cup \Omega_u} f_{Du} \ln(f_{Du}) dD du \tag{27}$$

Once again, the droplet velocity distribution is assumed to the delta function. In line with this assumption, the Lagrange multiplier method is used for constructing the f_D which exhibits the maximum Shannon entropy, given the constraints described in Eqs. 10, 14, and 18. This is given as:

$$f_D = 3\frac{D^2}{D_{30}^3} \exp\Big[-\lambda_0 - \lambda_1 \frac{D^3}{D_{30}^3} - \lambda_2 \frac{D_0}{D_{30}}\frac{D^2}{D_{30}^2}\Big] \tag{28}$$

where λ_0, λ_1, λ_2 are the unknown Lagrange multipliers and can be numerically solved by matching Eqs. 10, 14, and 18.

2.5 *The four-Lagrange-multiplier MEM model (referred to as MEM (4-Lag))*

The second MEM model takes the droplet velocity variations after the breakup into consideration. In this manner, we shall consider the constrains given in Eqs. 10 - 14. Then the maximum entropy method is used in conjunction with the Lagrange multiplier methods to determine f_{Du}, which gives us

$$f_{Du} = \frac{3}{u_0 D_{30}^3} D^2 \exp\Big[-\lambda_0 - \lambda_1 \frac{D^3}{D_{30}^3} - \lambda_2 \frac{D^3 u}{D_{30}^3 u_o} - \lambda_3 \Big(\frac{D^3 u^2}{D_{30}^3 u_o^2} + \frac{12}{We_{L,30}} \frac{D^2}{D_{30}^2} \Big) \Big] \quad (29)$$

The four unknown Lagrange multipliers, [λ_0 to λ_3], are numerically solved by matching Eqs. 10 - 14.

Having established f_{Du}, we can construct the droplet size distribution, $f_D(D) = \int_{\Omega_u} f_{Du} du$, which is a marginal density function of f_{Du} relating to droplet size. Likewise, integrating f_{Du} into determinations of droplet size yields the droplet velocity distribution, i.e. $f_u(u) = \int_{\Omega_D} f_{Du} dD$.

3 Assessment of model performance

For assessing the performances of the models, we consider the experimental data of Hsiang and Faeth [24], which gives the cumulative distribution percentage of the droplet volume as a function of D/MMD in the bag, multi-mode, and sheet thinning breakup regimes.

Fig. 1 features the comparisons between predicted values and the measured data. The best agreement is found for the four-Lagrange-multiplier MEM model (Eq. 29), followed by the three-Lagrange-multiplier MEM model (Eq. 28). The remaining three models (Eqs. 21, 22, and 24) do not yield reasonable agreement. This result also indicates that one underlying model assumption that the secondary droplet velocity is the same as that of the parent droplet is not appropriate.

As further validation, we check the predicted correlation between f_D and We_G. The attention is confined to the four-Lagrange-multiplier MEM model which exhibits the strongest agreement with the experimental measurements. In line with the results in Fig. 2a, when We_G increases, which is equivalent to the severity of atomization being intensified, the distribution of f_D skews to the left corresponding to a smaller mean value of D. In these circumstances, the normalization constraint of f_D, i.e. $\int_{\Omega_D} f_D dD = 1$, renders the peak value relatively high. The droplet velocity is distributed following a normal distribution centered at u_o, with a small mean value, as shown in Fig. 2b. When We_G increases, which pertains to a case where a larger u_o is present, the mean value of f_u increases while its peak value decreases.

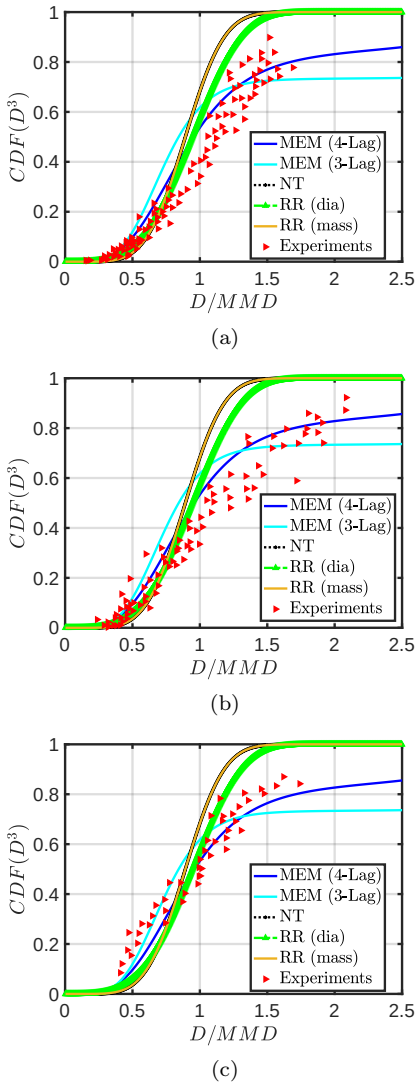

Figure 1: Comparison between the model predictions and the experimental measurements of Hsiang and Faeth [24]: (a) bag breakup (b) multi-mode breakup and (c) sheeting thinning breakup regimes. The estimations of the models are generated by giving We_G the values of 20, 60, and 100.

Conclusions

We propose five droplet breakup models for estimating the droplet size distribution of secondary droplet atomization. The model based on the maximum entropy method and which satisfies the conservations of mass, momentum, and energy is found to

exhibit the strongest agreement with the experimental measurements. This result also indicates that the prediction of the droplet size is affected by the density function of the droplet velocity, and the best prediction accuracy is reached when the droplet velocity distribution follows a normal distribution.

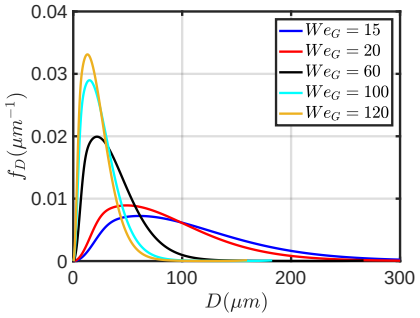

(a)

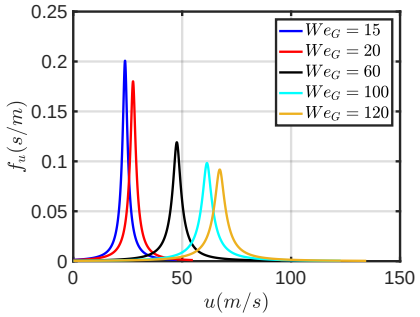

(b)

Figure 2: Marginal density functions of the four-Lagrange-multiplier MEM model: (a) droplet size, f_D, and (b) droplet velocity, f_u.

Acknowledgments

The support from the Caterpillar Corporation and the National Science Foundation (Number 1703825) is gratefully acknowledged.

References

[1] W.A. Sirignano. *Progress in Energy and Combustion Science*, 9(4):291–322, 1983.

[2] J. Heywood. *Internal combustion engine fundamentals*. McGraw-Hill Science, 1988.

[3] H.K. Chelliah. *Proceedings of the Combustion Institute*, 31(2):2711–2719, 2007.

[4] Y.M. Ferng and C.H. Liu. *Nuclear Engineering and Design*, 241(8):3142–3148, 2011.

[5] D. Nuyttens, M. De Schampheleire, P. Verboven, E. Brusselman, and D. Dekeyser. *Transactions of the ASABE*, 52(5):1471–1480, 2009.

[6] M. Knoche. *Crop protection*, 13(3):163–178, 1994.

[7] J.C. Beale and R.D. Reitz. *Atomization and sprays*, 9(6), 1999.

[8] P.J. O'Rourke and A.A. Amsden. *SAE Technical Paper*, 1987.

[9] R.D. Reitz. *Atomisation and Spray Technology*, 3(4):309–337, 1987.

[10] P. Rosin. *Journal of Institute of Fuel*, 7:29–36, 1933.

[11] H. Hiroyasu. *Topical Report, University of Wisconsin-Madison, 1967*, 1967.

[12] R.W. Sellens and T.A. Brzustowski. *Atomisation Spray Technology*, 1:89–102, 1985.

[13] X. Li and R.S. Tankin. *Combustion Science and Technology*, 56(1-3):65–76, 1987.

[14] C.E. Shannon. *Bell system technical journal*, 27(3):379–423, 1948.

[15] W.T. Kim, S.K. Mitra, X. Li, L.A. Prociw, and T.C.J. Hu. *Particle & Particle Systems Characterization*, 20(2):135–149, 2003.

[16] E. Movahednejad, F. Ommi, and S.M. Hosseinalipour. *Entropy*, 12(6):1484–1498, 2010.

[17] K. Yan, Z. Ning, M. Lü, and C. Sun. *Entropy*, 17(2):580–593, 2015.

[18] A. Bodaghkhani, B. Colbourne, and Y.S. Muzychka. *Ocean Engineering*, 155:106–114, 2018.

[19] S. Nukiyama and Y. Tanasawa. *Trans. Soc. Mech. Engrs.(Japan)*, 18:68–136, 1939.

[20] M. Jain, R.S. Prakash, G. Tomar, and R.V. Ravikrishna. *Proc. R. Soc. A*, 471(2177):20140930, 2015.

[21] H.C. Simmons. *Journal of Engineering for Power*, 99(3):309–319, 1977.

[22] J. Monaghan, G.A. Hill, and W.G. Soucey. *Defence Research Establishment Suffield Ralston (Alberta)*, 1981.

[23] P. González-Tello, F. Camacho, J.M. Vicaria, and P.A. González. *Powder Technology*, 186(3):278–281, 2008.

[24] L.P. Hsiang and G.M. Faeth. *International Journal of Multiphase Flow*, 18(5):635–652, 1992.